

# Microwave Absorption Characteristics of Conventionally Heated Nonstoichiometric Ferrous Oxide

ZHIWEI PENG, JIANN-YANG HWANG, JOE MOURIS, RON HUTCHEON,  
and XIANG SUN

The temperature dependence of the microwave absorption of conventionally heated nonstoichiometric ferrous oxide ( $\text{Fe}_{0.925}\text{O}$ ) was characterized *via* the cavity perturbation technique between 294 K and 1373 K (21 °C and 1100 °C). The complex relative permittivity and permeability of the heated  $\text{Fe}_{0.925}\text{O}$  sample slightly change with temperature from 294 K to 473 K (21 °C to 200 °C). The dramatic variations of permittivity and permeability of the sample from 473 K to 823 K (200 °C to 550 °C) are partially attributed to the formation of magnetite ( $\text{Fe}_3\text{O}_4$ ) and metal iron (Fe) from the thermal decomposition of  $\text{Fe}_{0.925}\text{O}$ , as confirmed by the high-temperature X-ray diffraction (HT-XRD). At higher temperatures up to 1373 K (1100 °C), it is found that  $\text{Fe}_{0.925}\text{O}$  regenerates and remains as a stable phase with high permittivity. Since the permittivity dominates the microwave absorption of  $\text{Fe}_{0.925}\text{O}$  above 823 K (550 °C), resulting in shallow microwave penetration depth ( $\sim 0.11$  and  $\sim 0.015$  m at 915 and 2450 MHz, respectively), the regenerated nonstoichiometric ferrous oxide exhibits useful microwave absorption capability in the temperature range of 823 K to 1373 K (550 °C to 1100 °C).

DOI: 10.1007/s11661-011-0652-9

© The Minerals, Metals & Materials Society and ASM International 2011

## I. INTRODUCTION

IN recent years, interest has grown rapidly in extending the application of microwave energy to the processing of a wide variety of new and engineered materials, including ceramics, polymers, composites, and chemicals.<sup>[1–3]</sup> However, the equations for the evaluation of the microwave absorption are complicated, especially for magnetic materials, and only a few investigators have paid close attention to the effect of temperature on the dielectric properties, which is extremely important for high-temperature materials processing under microwave irradiation.<sup>[4,5]</sup> As an important transitional material and precursor for various magnetic ceramic/metal nanocomposites or nanocrystals with high values of coercivity for the application as recording media, ferrous oxide has attracted much attention from researchers.<sup>[6–8]</sup> However, the absorption behavior of ferrous oxide under microwave irradiation has never been investigated.<sup>[9–11]</sup> Furthermore, some research claims that there is phase transformation due to thermal decomposition of ferrous oxide during the heating.<sup>[12,13]</sup> This interesting phenomenon may highly affect the characterization of the dielectric properties. Also, it is known that the microwave heating efficiency

of materials relies not only the dielectric properties but also on the magnetic properties. Although the ferrous oxide is known to be paramagnetic, and thus not a strong microwave absorber, the thermally decomposing heated sample may change substantially. Thus, a reasonable evaluation of microwave absorption capability of the ferrous oxide and its dissociation products should be based on the measurements of both permittivity and permeability.

The aim of this work is to measure the dielectric and magnetic properties of the nonstoichiometric ferrous oxide up to 1373 K and 823 K (1100 °C and 550 °C), respectively, using the cavity perturbation technique and to evaluate the temperature dependence of the microwave absorption capability of the ferrous oxide with consideration of the phase transformation during the heating.

## II. EXPERIMENTAL

Nonstoichiometric ferrous oxide powder samples (99 pct purity; they were fabricated starting with a higher iron oxide, then reducing the oxide by introducing iron metal) were purchased from Sigma-Aldrich (Sigma-Aldrich Corp., St. Louis, MO). The particle sizes, microstructure, and distribution of the oxides were characterized by a Hitachi S-4700 field-emission-scanning electron microscope (FE-SEM, Hitachi Ltd., Tokyo, Japan).

Room-temperature X-ray diffraction (RT-XRD) pattern for the sample was obtained using a conventional Scintag XDS2000 powder X-ray diffractometer (Scintag Inc., Cupertino, CA) with a graphite monochromator and  $\text{Cu K}\alpha$  radiation. The specific molecular formula of the oxide was determined by calculating the corresponding

ZHIWEI PENG, PhD Student, and JIANN-YANG HWANG, Professor, are with the Department of Materials Science and Engineering, Michigan Technological University, Houghton, MI 49931. Contact e-mail: jhwang@mtu.edu JOE MOURIS and RON HUTCHEON, Partners, are with Microwave Properties North (MPN), Deep River, ON K0J1P0, Canada. XIANG SUN, Postdoctoral Research Associate, is with Department of Mechanical, Aerospace and Nuclear Engineering, Rensselaer Polytechnic Institute, Troy, NY 12180.

Manuscript submitted October 13, 2010.

Article published online March 15, 2011

lattice parameter from the XRD pattern and comparing it with the JCPDS card.

The phase transformation of the sample during heating was identified by high-temperature X-ray diffraction (HT-XRD). The measurements were conducted in vacuum at 294 K, 373 K, 473 K, 573 K, 673 K, 773 K, 823 K, 873 K, 923 K, 973 K, 1273 K, and 1373 K (21 °C, 100 °C, 200 °C, 300 °C, 400 °C, 500 °C, 550 °C, 600 °C, 650 °C, 700 °C, 1000 °C and 1100 °C) using a PANalytical X'Pert PRO X-ray diffractometer (PANalytical B.V., Almelo, The Netherlands) with Cu  $K_\alpha$  radiation.

The permittivity and permeability of the sample were measured by the cavity perturbation technique, which is based on measuring the difference in the microwave cavity response between a cavity with a sample holder plus the sample.<sup>[14]</sup> The difference was then used to calculate either the permittivity or permeability, depending on the field type (electric or magnetic) in the region of the cavity in which the sample is placed. The high-temperature measurements were done by moving the hot sample and its holder rapidly from a conventional furnace into the high electric field (central) region of a thick-walled, well-cooled TM<sub>0n0</sub> cavity (Figure 1). The cavity mode frequency used in this experiment was  $915 \pm 0.5$  pct MHz or  $2450 \pm 0.5$  pct MHz and the detailed descriptions for the measurement fundamentals and the apparatus are found in the published literature.<sup>[14,15]</sup>

In the permittivity test, ferrous oxide powders passing the 0.1-mm screen were uniaxially pressed at about 172 MPa in a die lined with tungsten carbide to form three pellets with a diameter of about 4.03 mm and a total, stacked length (height) of 11.7 mm. The bulk density (room temperature) of the sample was 2.43 g/cm<sup>3</sup>. During the measurements, the sample was step heated in the conventional (resistance) furnace to the designated temperatures in 0.01 l/min flowing argon. The permittivity measurements started at 294 K (21 °C) and heated in 50 K to ~1373 K (50 °C to ~1100 °C). In

the permeability measurements, the same punch/die unit was used to form pellets with a diameter of about 4.03 mm and length of 12.6 mm. The bulk density of pellets (room temperature) was 2.59 g/cm<sup>3</sup>. The measurements were done in the same argon, starting at room temperature, then in 25 K (25 °C) steps to 823 K (550 °C).

### III. RESULTS AND DISCUSSION

The molecular formula of nonstoichiometric ferrous oxide was determined through the RT-XRD pattern (Figure 2), from which the lattice parameter was calculated. The ferrous oxide is identified as Fe<sub>0.925</sub>O (JCPDS card: 89-0686) with the lattice parameter of 4.036 Å using DMSNT software (Scintag Inc., Cupertino, CA).

Figure 3 presents the measured temperature dependence of permittivity involving the relative dielectric constant and the relative dielectric loss factor ( $\epsilon'_r$  and  $\epsilon''_r$ ,

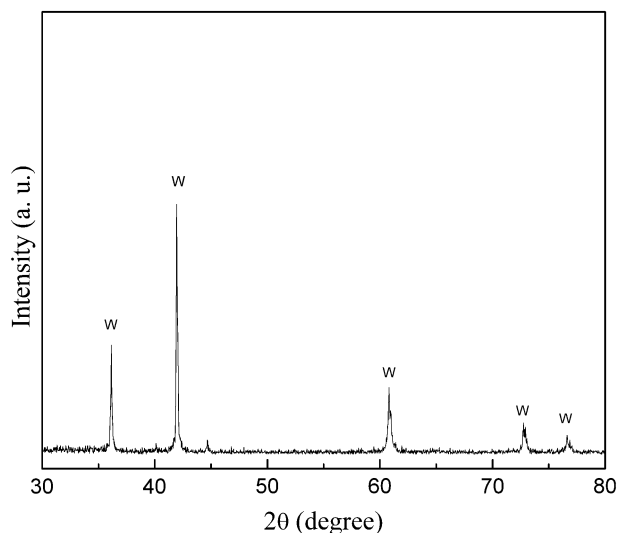


Fig. 2—RT-XRD pattern of the sample w-Fe<sub>0.925</sub>O.

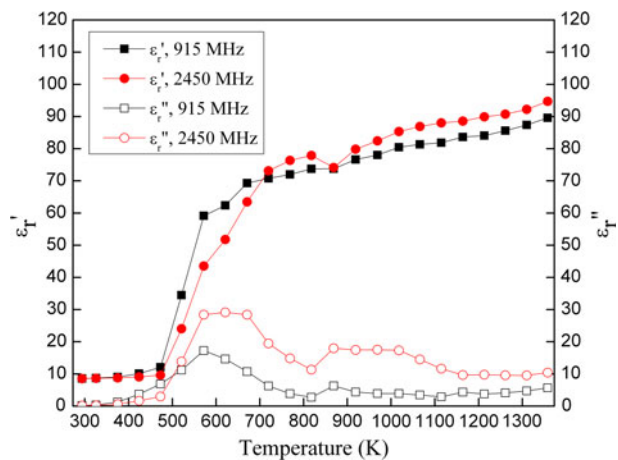


Fig. 3—Variation of complex relative permittivity of the sample as a function of temperature:  $\epsilon'_r$ —relative dielectric constant, and  $\epsilon''_r$ —relative dielectric loss factor.

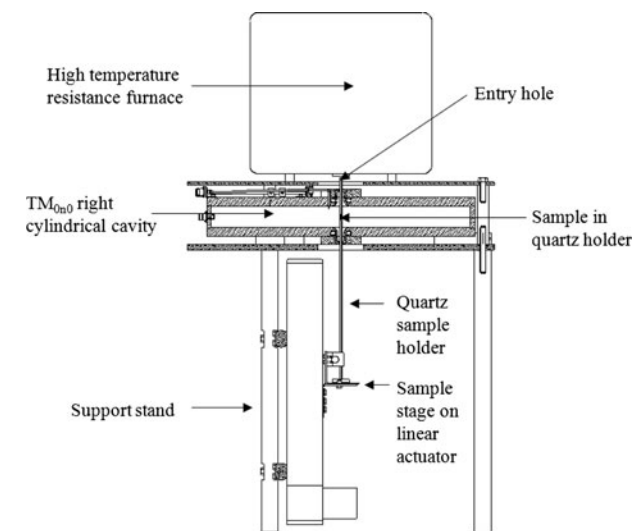


Fig. 1—Schematic diagram of the TM<sub>0n0</sub> cavity system (in cross section) showing the linear actuator with the quartz sample holder and a sample located on the axis in the center of the cavity.

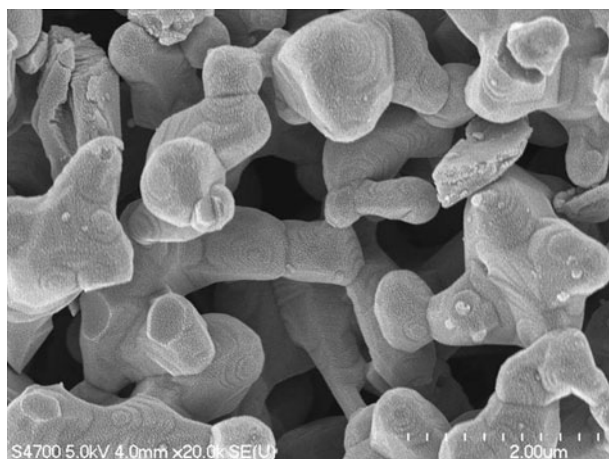
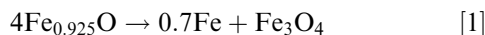


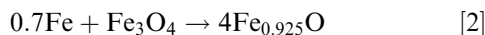
Fig. 4—Field emission-scanning electron microscope (FE-SEM) image of  $\text{Fe}_{0.925}\text{O}$  particles of 0.5- to 1.0- $\mu\text{m}$  size accumulating together and forming interstices between them.

respectively) of  $\text{Fe}_{0.925}\text{O}$ . The permittivity increases slightly along with temperature up to 473 K (200 °C), which is possibly associated with promotion of ionic diffusion with increasing temperature.<sup>[14]</sup> The FE-SEM image (Figure 4) shows that most particles of the sample are distributed in the size range of 0.5 to 1.0  $\mu\text{m}$ , and accumulate together and form interstices between them.

Note that  $\epsilon'_r$  increases dramatically between 473 K and 673 K (200 °C and 400 °C), while  $\epsilon''_r$  exhibits a dielectric loss peak in the range of 473 K to 823 K (200 °C to 550 °C). This is a typical relaxation/interfacial polarization phenomena behavior, usually indicating a change in the material associated with the loss of an insulating barrier between particles or the presence of a transient species during a phase change. In this case, it is expected to be mainly associated with the phase transformation resulting from the thermal decomposition of  $\text{Fe}_{0.925}\text{O}$ , which is clearly proved by the HT-XRD patterns shown in Figure 5. As revealed by the patterns, at temperatures below 473 K (200 °C), no phase change occurs. However, in the temperature range of ~573 K to 823 K (~300 °C to 550 °C), the peaks of magnetite and iron are observed, demonstrating the emergence of thermal decomposition of  $\text{Fe}_{0.925}\text{O}$ . Thus, the phase change probably contributes to the dramatic change of permittivity between 473 K and 823 K (200 °C and 550 °C). This observation is in agreement with previous research, which shows that the ferrous oxide is thermodynamically unstable below 848 K (575 °C), dissociating to metal and  $\text{Fe}_3\text{O}_4$ .<sup>[12,13,16]</sup> According to this investigation, the reaction can be expressed as follows:



As temperature continues to increase, the regeneration of the ferrous oxide occurs:



As displayed in Figure 5, the HT-XRD patterns of the sample exactly confirm these reactions. The peaks of

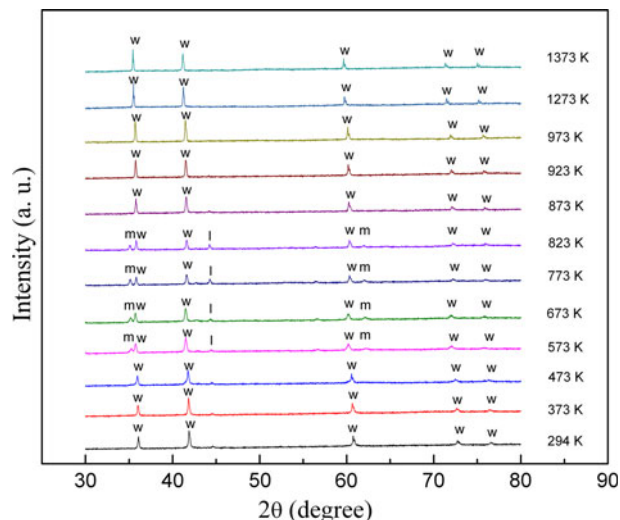


Fig. 5—HT-XRD patterns of the sample at various temperatures: w- $\text{Fe}_{0.925}\text{O}$ , m- $\text{Fe}_3\text{O}_4$ , and I-Fe.

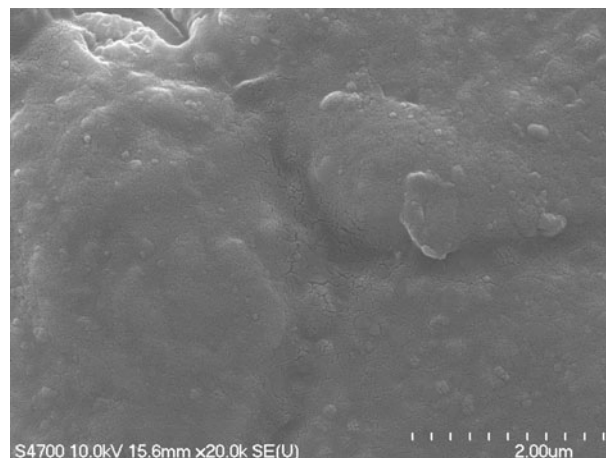


Fig. 6—FE-SEM image of  $\text{Fe}_{0.925}\text{O}$  after the dielectric measurement.

the magnetite and iron disappear at 873 K (600 °C). At even higher temperatures up to 1373 K (1100 °C),  $\text{Fe}_{0.925}\text{O}$  becomes quite stable. The relative dielectric constant continues to increase in this stage with a much slower rate. The relative dielectric loss factor remains almost stable between 873 K and 1073 K (600 °C and 800 °C) and then decreases a little up to 1373 K (1100 °C). This may be associated with the “sintering effect,” which occurred during the heating at high temperature, as revealed by the FE-SEM microstructure image (Figure 6) of the heated product after the dielectric measurement. In fact, the sintering occurring at the temperature above 1273 K (1000 °C) makes the particles adhere to each other. During this process, densification and grain growth were observed and the decrease of the porosity in the sample and increase of the average grain size were noticed, which hinders the diffusions of iron and oxygen ions,<sup>[17]</sup> possibly influencing the microwave absorption capability in this temperature range.



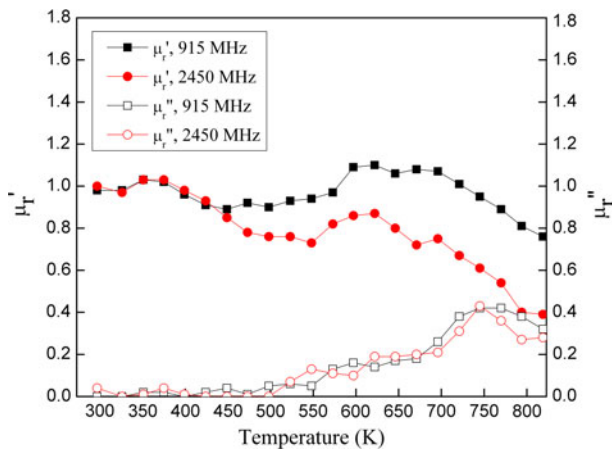


Fig. 7—Variation of complex relative permeability of the sample as a function of temperature:  $\mu_r'$ —relative magnetic constant, and  $\mu_r''$ —relative magnetic loss factor.

Figure 7 describes the variation of complex relative permeability of the sample as a function of temperature. At the temperature below  $\sim 473$  K ( $\sim 200$  °C), the relative magnetic constant and magnetic loss factor ( $\mu_r'$  and  $\mu_r''$ , respectively) are around 1 and 0, respectively. This finding indicates that the nonstoichiometric ferrous oxide exhibits little magnetism, which is in agreement with the paramagnetism it exhibits at room temperature. As the temperature increases, the magnetic loss gradually grows likely due to the formation of iron and magnetite from the thermal decomposition of the ferrous oxide, as discussed previously. The metal Fe (ferromagnetic) and  $\text{Fe}_3\text{O}_4$  (ferrimagnetic) formed after the decomposition are expected to contribute to the substantial increase of relative magnetic loss factor. However, this trend changes at a temperature of around 823 K (550 °C), which is probably related both to the “Curie point” effect, where  $\text{Fe}_3\text{O}_4$  loses magnetism, and to the reproduction of  $\text{Fe}_{0.925}\text{O}$ .<sup>[16]</sup> Thus, the thermal decomposition of  $\text{Fe}_{0.925}\text{O}$  hinders the determination of the dielectric and magnetic properties of “true”  $\text{Fe}_{0.925}\text{O}$  from  $\sim 473$  K to  $\sim 823$  K ( $\sim 200$  °C to  $\sim 550$  °C). At the temperature higher than 823 K (550 °C), however, this “disturbance” can be excluded due to the regeneration of nonstoichiometric ferrous oxide. This observation also implies that a low magnetic loss of the ferrous oxide could be estimated at temperatures above 823 K (550 °C), although the experiment did not continue the permeability measurement in this range. Moreover, it should be mentioned that the relative magnetic constant decreases during the decomposition process. This is because the magnetic response of materials depends on the saturation magnetization, which decreases with increasing temperature.<sup>[18]</sup> The conversion to magnetite does turn on a ferrimagnetic response, but it decreases with temperature eventually.

The characterization of the microwave propagation behavior of materials should use both the permittivity and permeability to determine the microwave attenuation. However, many researchers use the penetration depth ( $D_p$ ) as written in Eq. [3], considering only the

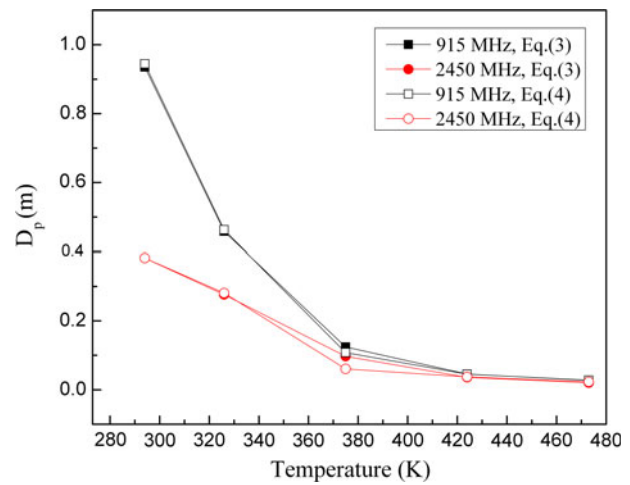


Fig. 8—Microwave penetration depth of  $\text{Fe}_{0.925}\text{O}$  in the temperature range of 294 K to 473 K (21 °C to 200 °C).

permittivity (since the use of the full formulation with permeability is difficult, and also the permeability data may not be available):<sup>[19]</sup>

$$D_p = \frac{\lambda_0}{2\pi(2\epsilon_r')^{1/2}} \left\{ \left[ 1 + \left( \frac{\epsilon_r''}{\epsilon_r'} \right)^2 \right]^{1/2} - 1 \right\}^{-1/2} \quad [3]$$

where  $\lambda_0$  is the microwave wavelength in free space. The evaluation of the microwave absorption based on Eq. [3] may be in serious error for magnetic dielectrics. To solve this problem, the authors have derived a new equation for the penetration depth (including permittivity and permeability), which is easier to use:<sup>[20]</sup>

$$D_p = \frac{\lambda_0}{2\sqrt{2}\pi} \left\{ \epsilon_r''\mu_r'' - \epsilon_r'\mu_r' + \left[ (\epsilon_r'\mu_r')^2 + (\epsilon_r''\mu_r'')^2 + (\epsilon_r'\mu_r'')^2 + (\mu_r'\epsilon_r'')^2 \right]^{1/2} \right\}^{-1/2} \quad [4]$$

Figure 8 reveals little difference between the penetration depths calculated by Eqs. [3] and [4] from 294 K to 473 K (21 °C to 200 °C). In this low-temperature range, the tiny magnetic loss factor of  $\text{Fe}_{0.925}\text{O}$  presents little effect on the penetration depth, while the increase of permittivity (actually, the dielectric loss factor,  $\epsilon_r''$ ) results in a rapid decrease of penetration depth along with temperature. The small penetration depth (less than 0.03 m for both frequencies at 473 K (200 °C)) also implies that  $\text{Fe}_{0.925}\text{O}$  exhibits strong microwave absorption capability at a relatively low temperature. At temperatures between 473 K and 823 K (200 °C and 550 °C), the phase change due to thermal decomposition of  $\text{Fe}_{0.925}\text{O}$  influences the determination of penetration depth of  $\text{Fe}_{0.925}\text{O}$ , but it still can be expected that the permittivity dominates the microwave absorption of the sample because of much higher complex relative permittivity than the complex relative permeability. This can be proved further by the microwave penetration depth of the sample at temperatures above 823 K

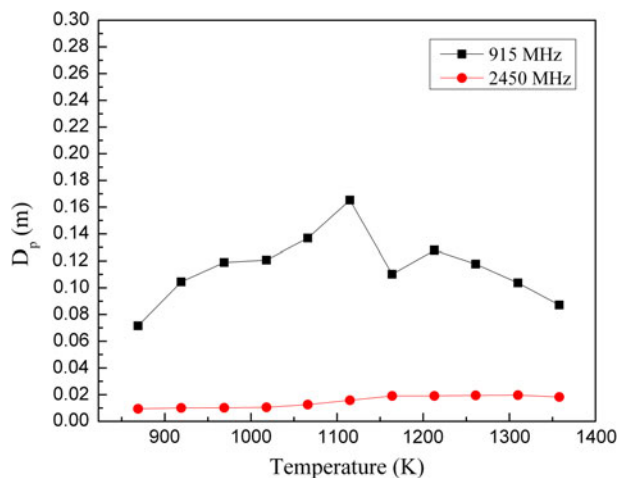


Fig. 9—Microwave penetration depth of  $\text{Fe}_{0.925}\text{O}$  at temperatures between 823 K and 1373 K (550 °C and 1100 °C).

(550 °C), as shown in Figure 9. In this temperature range, it is reasonable to neglect the influence of permeability since the relative permittivity is so high, and the strength of paramagnetism decreases with temperature. It is found that the penetration depth remains almost constant ( $\sim 0.11$  and  $\sim 0.015$  m at 915 and 2450 MHz, respectively) in this range, indicating the quite stable phase composition (actually, pure  $\text{Fe}_{0.925}\text{O}$ ) in the measurement, which is in agreement with the HT-XRD pattern of the product after heating. Note that the penetration depth at 915 MHz is relatively longer than that at 2450 MHz mainly due to the apparent difference between the microwave wavelengths ( $\lambda_0$ ) at these frequencies rather than the frequency dependencies of permittivity and permeability. (At both frequencies, the permittivity and permeability show the similar variation trends and close values with increasing temperature.) The shallow microwave penetration depths indicate that the nonstoichiometric ferrous oxide presents useful microwave absorption capability between 823 K and 1373 K (550 °C and 1100 °C).

#### IV. CONCLUSIONS

As an important transitional phase and precursor for various advanced magnetic materials, a type of nonstoichiometric ferrous oxide ( $\text{Fe}_{0.925}\text{O}$ ) was employed to investigate its microwave absorption capability based on the measurements of the permittivity and permeability using the cavity perturbation technique. The values of permittivity of the nonstoichiometric ferrous oxide increase as the temperature increases from 294 K to 473 K (21 °C to 200 °C). The metal iron and magnetite formed from the thermal decomposition of  $\text{Fe}_{0.925}\text{O}$

exert some influence on the variation of permittivity and permeability of the sample between 473 K and 823 K (200 °C and 550 °C), complicating the evaluation of microwave absorption behaviors of  $\text{Fe}_{0.925}\text{O}$ . At even higher temperatures,  $\text{Fe}_{0.925}\text{O}$  starts to regenerate and becomes quite stable. The calculated penetration depth of microwave demonstrates that the ferrous oxide manifests useful microwave absorption capability in the temperature range of 823 K to 1373 K (550 °C to 1100 °C).

#### ACKNOWLEDGMENTS

The authors graciously appreciate the financial support from the Michigan Public Service Commission, U.P. Steel, and the United States Department of Energy (DOE). The authors also thank Microwave Properties North ([www.mpn.ca](http://www.mpn.ca)) for performing the permittivity and permeability measurements.

#### REFERENCES

1. Y.V. Bykov, K.I. Rybakov, and V.E. Semenov: *J. Phys. D: Appl. Phys.*, 2001, vol. 34, pp. R55–R75.
2. Y. Fang, J. Cheng, and D.K. Agrawal: *Mater. Lett.*, 2004, vol. 58, pp. 498–501.
3. Q. Yang, H. Zhang, Y. Liu, Q. Wen, and L. Jia: *Mater. Lett.*, 2008, vol. 62, pp. 2647–50.
4. D.M. Mingos and D.R. Baghurst: *Chem. Soc. Rev.*, 1991, vol. 20, pp. 1–47.
5. E.T. Thostenson and T.W. Chou: *Appl. Sci. Manuf.*, 1999, vol. 30, pp. 1055–71.
6. M. Yin, Z. Chen, B. Deegan, and S. O'Brieh: *J. Mater. Res.*, 2007, vol. 22, pp. 1987–95.
7. M. Gheisari, M. Mozaffari, M. Acet, and J. Amighian: *J. Magn. Magn. Mater.*, 2008, vol. 320, pp. 2618–22.
8. M. Mozaffari, M. Gheisari, M. Niyafar, and J. Amighian: *J. Magn. Magn. Mater.*, 2009, vol. 321, pp. 2981–84.
9. L. Takacs: *Nanostruct. Mater.*, 1993, vol. 2, pp. 241–49.
10. J. Ding, W.F. Miao, E. Pirault, R. Street, and P.G. McCormick: *J. Alloy. Compd.*, 1998, vol. 267, pp. 199–204.
11. K. Tokumitsu and T. Nasu: *Scripta Mater.*, 2001, vol. 44, pp. 1421–24.
12. B. Andersson and J.O. Sletnes: *Acta Cryst.*, 1977, vol. A33, pp. 268–76.
13. L. Broussard: *J. Phys. Chem.*, 1969, vol. 73, pp. 1848–54.
14. C.A. Pickles, J. Mouris, and R. Hutcheon: *J. Mater. Res.*, 2005, vol. 20, pp. 18–29.
15. R.M. Hutcheon, M. de Jong, and F.P. Adams: *J. Microwave Power E.*, 1992, vol. 27, pp. 93–102.
16. H. Shechter and P. Hillman: *J. Appl. Phys.*, 1966, vol. 37, pp. 3043–47.
17. D. Zhang, G. Weng, S. Gong, and D. Zhou: *Mater. Sci. Eng. B: Adv.*, 2003, vol. 99, pp. 428–32.
18. E.D. Thompson, E.P. Wohlfarth, and A.C. Bryan: *Proc. Phys. Soc.*, 1964, vol. 83, pp. 59–70.
19. A.C. Metaxas and R.J. Meredith: *Industrial Microwave Heating*, Peter Peregrinus, London, 1983, pp. 80–81.
20. Z. Peng, J.Y. Hwang, J. Mouris, R. Hutcheon, and X. Huang: *ISIJ Int.*, 2010, vol. 50, pp. 1590–96.